Magnetic Resonance Imaging of the Distant Dipolar Field in Structured Samples Using Intermolecular Multiple-Quantum Coherences of Various Orders

L. Bouchard[1], X. Tang[1], C. Chin[2], F. W. Wehrli[2], W. S. Warren[1]

[1]Princeton University, Princeton, New Jersey, United States, [2]University of Pennsylvania, Philadelphia, Pennsylvania, United States

Synopsis. Intermolecular multiple-quantum coherences (iMQC) have been proposed as a novel contrast mechanism for clinical MRI. Its reliance on the distant dipolar field offers a user-tunable distance scale over which tissue structure can be probed. The potential for functional MRI, tumor detection and measurements of trabecular bone architecture have drawn considerable attention. We demonstrate that an 8-step phase cycle can be used to simultaneously extract images corresponding to several quantum coherence pathways, each potentially containing a wealth of information to help characterize the microstructure.

Introduction. In a perfectly homogeneous solution, the coherence pathway selection of a two-quantum CRAZED experiment is very accurate. In a highly structured sample such as trabecular bone [1], fast-moving blood in a vein or artery, or packed beads, the spatial averaging which eliminates odd-symmetry terms in the density matrix and terms which depend on absolute position is partially invalidated due to geometric interfaces and boundaries. Consequently, zero (ZQC), single (SQC) or higher order quantum coherences may leak out and contaminate the signal from an iMQC sequence even if an M:1 ratio of gradient areas is used. Fortunately, rf phase cycling may be added to select the desired coherence pathway while blocking unwanted pathways. It may be shown that, in order to uniquely select the M^{th} quantum order, a receiver phase φ_{REC} of $\Phi_B\cdot(\Phi_A/\Phi_B)^M$ must be selected, where Φ_A and Φ_B are the phase factors of the first and second rf pulses, respectively, for an 8 steps phase cycling scheme.

Ex	SQC	DQC	TQC
1	0	0	0
2	7π/4	3π/2	5π/4
3	3π/2	π	π/2
4	5π/4	π /2	7π/4
5	π	0	π
6	3π/4	3π/2	π/4
7	π/2	π	3π/2
8	π/4	π/2	3π/4

Table 1. Receiver phase cycles.

Methods. MR images were acquired at 4T on a GE Signa scanner equipped with a 3.4-cm diameter solenoidal home built probe. A two-quantum MODCRAZED [2] sequence (τ=40ms, TE=300ms, TR=5s, Thk=10mm, 64×64 matrix, 4cm FOV, RBW=2 kHz, correlation gradient (0.1 G/cm for 7ms) along the slice thickness perpendicular to B_0). The phase of the second rf pulse was kept fixed at 2π rad., while that of the first rf pulse was cycled from 0 to 7π/4 in steps of π/4. Non-selective BIR-4 excitation and hyperbolic secant refocusing pulses were used to produce uniform excitations across the sample. Fig. 1 shows a proton-density weighted GRE scan of the 10mm slice which is centered on five 8mm-diameter plastic balls. Small portions of balls lying partially in the slice can also be seen.

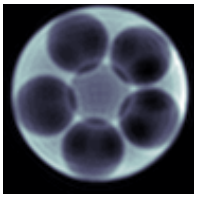

Fig 1. GRE control image.

Results and Discussion. Selection of the positive SQC pathway requires adding the 8 excitations while cycling the receiver phase according to the sequence shown in Table 1. Positive DQC and TQC pathways are chosen in a similar way. Negative quantum pathways are selected by taking the complex conjugate phase of its positive counterpart in Table 1. Magnetic resonance images corresponding to the M=±1, ±2, ±3 quantum coherences are shown in Fig. 2. All images are scaled to their maximum intensity and acquired using the same tuning and receiver gain for comparison. The SQC images contain contributions from single-spin and multi-spin terms with the former being the most intense. SQC leakage arises from incomplete helix cycles across the slice thickness as well as due to the interface boundary of the plastic balls. Rings of varying intensity can be seen as the thickness of the ball (the so-called "height" function) varies smoothly with position. Variation of the first rf pulse phase in smaller steps (π/64) to increment the absolute phase of the magnetization helix revealed this transition is gradual (not shown here). This confirmed that the SQC rings were due to the ball interface. In a similar way, the intensity of the background water signal (outside the balls) could be attributed at least partly to incomplete helix cycles at the edge of the slice boundaries. The overall difference in intensity between +SQC and –SQC is mainly due to the different helix pitch for each case (in a 3:1 ratio) giving rise to a different amount of leakage.

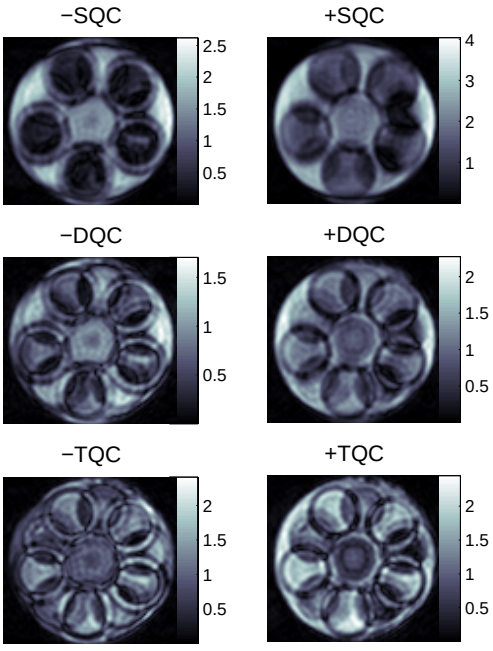

Fig 2. MODCRAZED iMQC images of +/- single, double and triple quantum coherence pathways.

DQC and TQC images involve 2 or more spin interactions, which are separated by the correlation distance (Dc=1.70 mm, in our case) and so the image contrast is expected to be different than SQC. As is best seen for the TQC case (Fig. 2), balls lying in the adjacent slices are readily seen. Such contrast based on long-range dipolar interaction is fundamentally different from conventional SQC image contrast.

Conclusion. In a highly structured sample, simple gradient refocusing is not sufficient to select a particular order of iMQC. For clinical imaging, care must be taken to use the correct phase cycling scheme to select the desired order. The image contrast obtained from the various pathways has a different functional dependence than conventional images. In particular, DQC and TQC images are strongly sensitive to long-range interactions. The distance scale of these interactions can be tuned to provide potentially useful image contrast for clinical applications.

References. [1] S. Capuani, MRM 46:683 (2001) [2] S. Garrett-Roe, JMR 146, 1-13 (2000)